

# On the mystery of the perennial carbon dioxide cap at the south pole of Mars

Xin Guo,<sup>1</sup> Mark Ian Richardson,<sup>2</sup> Alejandro Soto,<sup>1</sup> and Anthony Toigo<sup>3</sup>

Received 18 March 2009; revised 14 August 2009; accepted 6 October 2009; published 9 April 2010.

[1] A perennial ice cap has long been observed near the south pole of Mars. The surface of this cap is predominantly composed of carbon dioxide ice. The retention of a CO<sub>2</sub> ice cap results from the surface energy balance of the latent heat, solar radiation, surface emission, subsurface conduction, and atmospheric sensible heat. While models conventionally treat surface CO<sub>2</sub> ice using constant ice albedos and emissivities, such an approach fails to predict the existence of a perennial cap. Here we explore the role of the insolation-dependent ice albedo, which agrees well with Viking, Mars Global Surveyor, and Mars Express albedo observations. Using a simple parameterization within a general circulation model, in which the albedo of CO<sub>2</sub> ice responds linearly to the incident solar insolation, we are able to predict the existence of a perennial CO<sub>2</sub> cap at the observed latitude and only in the southern hemisphere. Further experiments with different total CO<sub>2</sub> inventories, planetary obliquities, and surface boundary conditions suggest that the location of the residual cap may exchange hemispheres favoring the pole with the highest peak insolation.

**Citation:** Guo, X., M. I. Richardson, A. Soto, and A. Toigo (2010), On the mystery of the perennial carbon dioxide cap at the south pole of Mars, *J. Geophys. Res.*, 115, E04005, doi:10.1029/2009JE003382.

## 1. Introduction

[2] Carbon dioxide (CO<sub>2</sub>) is the leading gaseous species on Mars, comprising 95% of the atmosphere [Owen *et al.*, 1977]. Throughout a Martian year, up to 30% of the total CO<sub>2</sub> condenses on the surface in the winter polar region and forms frost caps [Kelly *et al.*, 2006; Tillman *et al.*, 1993]. While the discovery of seasonal ice caps at the poles of Mars dates back to the eighteenth century, the existence of a perennial (or residual) CO<sub>2</sub> ice cap at the south pole of Mars was first discovered by the Viking spacecraft [Byrne and Ingersoll, 2003; Kieffer *et al.*, 1977; Kieffer, 1979; Paige *et al.*, 1990]. The south residual cap also contains a small area of exposed water ice [Bibring *et al.*, 2004].

[3] The annual CO<sub>2</sub> cycle on Mars can be explained by the varying components in the surface energy balance of the caps, including the latent heat exchange, solar radiation, surface emission, subsurface conduction, and atmospheric sensible heat [Guo *et al.*, 2009; Paige, 1992; Wood and Paige, 1992]. Ideally, general circulation models (GCMs) should be able to simultaneously predict the atmospheric budget and the surface budget of CO<sub>2</sub> correctly, e.g., fitting the Viking Lander (VL) pressure cycle while reasonably

predicting the CO<sub>2</sub> caps' (including seasonal and perennial caps) existence and behaviors. Indeed, most GCMs are able to fit the atmospheric budget and the seasonal caps reasonably well by tuning the seasonal cap albedos and emissivities, the total CO<sub>2</sub> inventory in the system, and the subsurface thermal properties [Forget *et al.*, 1999; Guo *et al.*, 2009; Haberle *et al.*, 2008; Kelly *et al.*, 2006; Pollack *et al.*, 1993]. However, simulating the residual CO<sub>2</sub> cap remains more challenging because simple energy balance models (and all published GCM results) do not predict its existence; more accurately, the time-invariant albedo and emissivity values preferentially chosen to fit the VL pressure cycles are not able to support a residual CO<sub>2</sub> cap in the southern summer. GCMs understandably give priority to fitting the atmospheric budget because of the induced seasonal pole-to-pole flow and because of the influence of total mass variations on other components of the circulation and climate. Paige and Ingersoll [1985] suggest that the only reason that the southern residual cap can endure the southern summer is the very high albedo it attains near solstice. These late season southern cap albedos are much higher than those used in GCMs to obtain good fits to the CO<sub>2</sub> cycle, especially for the southern cap.

[4] Wood and Paige [1992] suggest that in order to maintain the southern residual cap a higher albedo or a higher emissivity or both is required. While one finds little evidence supporting the idea that CO<sub>2</sub> ice emissivity is very different from unity [Forget *et al.*, 1998; Haberle *et al.*, 2008] except for the "cryptic" regions [Kieffer, 1979; Kieffer *et al.*, 2000], there is abundant evidence that the albedo of the CO<sub>2</sub> ice changes: Viking Orbiter observations suggest

<sup>1</sup>Planetary Science, Division of Geological and Planetary Sciences, California Institute of Technology, Pasadena, California, USA.

<sup>2</sup>Ashima Research, Pasadena, California, USA.

<sup>3</sup>Center for Radiophysics and Space Research, Cornell University, Ithaca, New York, USA.

that the albedo of the southern residual cap changes with time [James *et al.*, 1992; Paige and Ingersoll, 1985], while the Thermal Emission Spectrometer (TES), the Mars Orbiter Laser Altimeter (MOLA), and the Observatoire pour la Minéralogie, l'Eau, les Glaces, et l'Activité (OMEGA) also found evidence that the albedo of the seasonal caps evolves [Byrne *et al.*, 2008; Kieffer *et al.*, 2000; Kieffer and Titus, 2001; Schmidt *et al.*, 2009]. These changes are of unknown origin but are possibly related to microphysical processes, such as dust–ice interaction, frost grain size evolution with insolation, and surface roughness change due to sublimation [Ingersoll *et al.*, 1992]. Schmidt *et al.* [2009] suggest that the CO<sub>2</sub> sublimation in the southern polar cap is mainly controlled by albedo at both global and local scales. More interestingly, the Viking observations suggest that the residual CO<sub>2</sub> cap albedo responds to the incident solar flux in a very linear way. This relationship is likely key to explaining the existence of the perennial cap [Paige, 1985].

[5] Given the complete failure of constant albedo models to predict a residual CO<sub>2</sub> ice cap at the south, this study is focused on asking whether the introduction of an insolation-dependent albedo of CO<sub>2</sub> ice can predict such a cap. The residual cap is largely irrelevant to the current climate insofar as it lacks sufficient mass to consequentially buffer the atmosphere, but this may not have been true at various earlier stages of Martian climate history. The triggering of cap formation at different values of obliquity, orbital parameters, and total CO<sub>2</sub> reservoir and questions relating to the timing of atmospheric collapse for thicker atmospheric states will be of consequence for understanding plausible paleoclimatic states. For situations in which the occurrence of residual ice caps is of interest, it would seem that being able to predict a perennial CO<sub>2</sub> ice cap for the current climate would be a prerequisite test for any model. We thus undertake an initial exploration of how the insolation-dependent albedo influences residual cap development for these parameters.

[6] We perform a systematic study using a Mars GCM, the planetary Weather Research and Forecasting (WRF) model, to explore the possible environments conducive to perennial CO<sub>2</sub> cap formation. We perform simulations with and without insolation-dependent albedo in order to isolate the effect of varying albedo as observed. We also explore the effects of different total CO<sub>2</sub> inventory, different planetary obliquity, and different topographic setups. Section 2 provides an introduction to the WRF model, and then we present the model results in section 3, followed by discussions and conclusions in section 4.

## 2. Model Description and Setup Description

[7] In this paper, we use the MarsWRF model, the Martian implementation of the PlanetWRF model [Richardson *et al.*, 2007]. A typical 3-D setup of MarsWRF contains a grid structure yielding 36 × 64 × 40 (latitude, longitude, vertical) points. This setting provides a global coverage of Mars with the top of the model reaching up to 0.006 Pa, or about 80 km above the surface. Its horizontal resolution is 5.0° of latitude by 5.6° of longitude. Broadband radiative calculations cover visible and infrared spectral regions with climatological aerial dust backgrounds. Boundary condi-

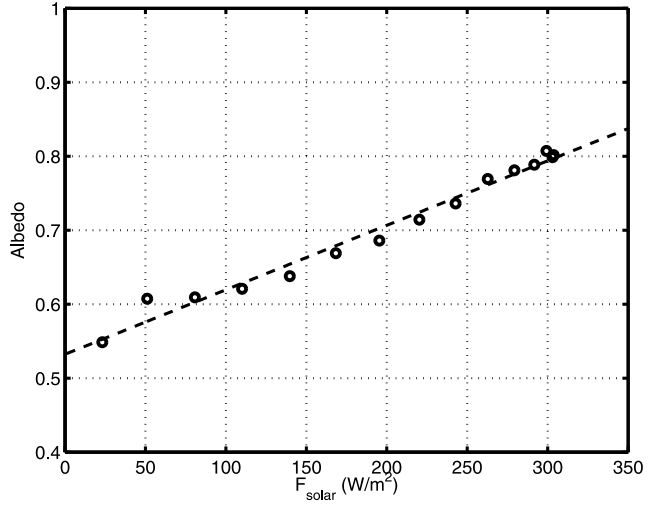


**Figure 1.** Southern residual cap albedo as a function of incident solar insolation. Open circles are observations from the infrared thermal mapper on the Viking orbiter [James *et al.*, 1992]. Dashed line is the line from the linear fitting of the Viking data (equation (1)).

tions, including topography, surface albedo, thermal inertia, terrain slope, and slope orientation, are taken from space-craft measurements (mostly from Mars Global Surveyor). Though simple treatment of atmospheric CO<sub>2</sub> condensation is included, water cycle and CO<sub>2</sub> cloud microphysics, which are likely aliased to the model parameterization of frost albedo and emissivity [Guo *et al.*, 2009], are not explicitly calculated. The temperature at the lower boundary of the subsurface layer is obtained from previous long-term simulations and stays fixed. Therefore, the subsurface reaches thermal equilibrium in a relatively short period of time (usually less than 100° of solar longitude ( $L_s$ )). Nevertheless, data starting at the second year (after 360° of  $L_s$ ) are used for the analysis in this paper.

[8] We calibrate the GCM by tuning the albedos and the emissivities of the seasonal dry ice caps and the total CO<sub>2</sub> inventory in the system to reproduce the VL1 surface pressure cycles. At the steady state, the model predicts a pressure cycle that matches the Viking Lander records very closely [Guo *et al.*, 2009]. The predicted mass of the seasonal caps is consistent with other GCMs and observations [Kelly *et al.*, 2006]. However, like all the other models trying to fit the VL pressure records, a residual CO<sub>2</sub> cap in the south pole is not predicted by MarsWRF with this setup (as a side note, most models include the thermal effects of a residual ice cap by “hard wiring” surface temperature at the south pole to the CO<sub>2</sub> condensation point).

[9] Spacecraft observations suggest that the albedo of the southern residual CO<sub>2</sub> cap changes with time, and this relationship is most amenably expressed with the Viking infrared thermal mapper data as shown by James *et al.* [1992] using data from Paige and Ingersoll [1985]. The observed relationship between the residual CO<sub>2</sub> cap's albedo and the incident solar flux is very linear (Figure 1). When we use a least squares linear regression method, we

obtain an empirical equation that predicts the surface CO<sub>2</sub> frost albedo on the basis of the insolation:

$$A = 0.532 + 8.72 \times 10^{-4} \times F_s, \quad (1)$$

where  $A$  is the albedo of the CO<sub>2</sub> ice cap and  $F_s$  is the incident solar flux in W m<sup>-2</sup>. This linear model fits the Viking albedo observations for the southern residual cap very well, with only several percent of fitting error. In the absence of a proven physical model for the dependence of albedo on insolation or other environmental factors, this empirical relationship is potentially very important for reproducing a perennial cap in a GCM. For a given emissivity and fixed temperature, a larger albedo creates a larger energy deficit that has to be compensated by more surface CO<sub>2</sub> ice condensation or less sublimation. Equation (1) implies that the albedo is the largest in the summer when the incident solar flux is the most intense, which is ideal for the CO<sub>2</sub> ice to endure the summer.

[10] We incorporated this relationship into MarsWRF. For each time step, if the surface is covered by enough CO<sub>2</sub> ice (for all simulations, a threshold mass coating of CO<sub>2</sub> ice is required in the GCM for modification of the albedo; the value is chosen such that the albedo is changed only when the abundance of CO<sub>2</sub> ice can reasonably be expected to dominate the reflection of sunlight over the scale of a grid cell), we calculate the instantaneous incident solar flux and then use equation (1) to determine the surface albedo for the subsequent radiative calculations (of course, the albedo value cannot be larger than unity). We also experimented with different total CO<sub>2</sub> inventories and different obliquities and undertook sensitivity studies to determine the influence of topography, thermal inertia distribution, and other factors on the existence and location of the residual cap. Results of model runs are shown in section 3. In all cases, output from the second year of model simulations is shown.

### 3. Model Results

#### 3.1. Control Case: Constant Albedo, Current CO<sub>2</sub>, and Orbital Parameters

[11] We first present the control or baseline scenario with a time-constant albedo. Time-constant albedos and emissivities are assigned to the northern and southern CO<sub>2</sub> ice caps. The total CO<sub>2</sub> mass in the system was set to  $2.83 \times 10^{16}$  kg [Guo et al., 2009]. As mentioned in section 2, this setup generates a pressure cycle at the VL1 location agreeing with the VL1 records very well but without a CO<sub>2</sub> residual cap at either pole. The annual variation of the zonally averaged surface CO<sub>2</sub> frost is shown in Figure 2a.

#### 3.2. Albedo Responses to Solar Insolation

[12] Next we show an experiment in which the surface CO<sub>2</sub> ice albedo is determined from the local incident solar flux according to equation (1) while keeping the rest of the model unchanged (note that the albedo of CO<sub>2</sub> ice present at any location on the surface is locally determined by this formula). We show the corresponding CO<sub>2</sub> ice surface deposition annual cycle in Figure 2b.

[13] Following the seasonal cap evolution, starting with the onset of polar night in each hemisphere, CO<sub>2</sub> begins to

deposit at the winter poles. At this time of the year, the seasonal cap areal coverage in both hemispheres does not differ greatly in the time-varying albedo experiment compared to the control case. This is expected because during the polar nights the surface albedo is not relevant to the surface energy balance. When the surface frost is exposed to the Sun, the abundance and the longevity of the surface CO<sub>2</sub> ice starts to differ from the control case. In the northern hemisphere, the albedo determined by equation (1) is usually comparable or slightly smaller than the value used in the control case. As a result, the CO<sub>2</sub> ice in the north in the varying albedo case sublimates at the same rate or slightly faster than in the control case. More dramatic change can be found in the southern hemisphere. As the southern seasonal ice cap is exposed to sunlight as the spring wears on, the albedo is driven to higher values than in the north and to higher values than those used in the south in the control simulation. This brightening of the southern cap leads to less solar energy absorption and thus reduces the cap sublimation rate. Indeed, thanks to the high albedos generated by equation (1), the CO<sub>2</sub> ice at the southern pole is able to endure the summer and forms a perennial reservoir.

[14] The reason for the existence of perennial CO<sub>2</sub> ice in the GCM is consistent with *Paige and Ingersoll's* [1985] study of the heat balance of the residual cap. The perennial ice reservoir produced by the GCM is slightly displaced from the geographical south pole and is longitudinally asymmetric, in common with the observations [*Colaprete et al.*, 2005; *Kieffer et al.*, 1977]. However, the model-generated cap is not located at the correct longitudes. The observed southern residual cap is confined in the area between 84°S and 90°S, tilted toward 300°E longitude; our simulation has only one grid point representing the residual cap centered at 81.2°S and 73°E (Figure 3). We will have further discussion about this asymmetry in section 3.6.

[15] It should be noted that the use of equation (1) to determine albedo for any and all CO<sub>2</sub> surface ice deposits introduces an error into the fitting of the VL pressure curves. As we stated in section 2, equation (1) was derived from a data set only for the area of the residual CO<sub>2</sub> cap, and its applicability to the whole planet is questionable. Indeed, it seems that geology and the history of the nature of the ice deposition (whether direct surface deposition or snowfall) influence the geographical distribution of the albedo-insolation relationship [*Colaprete et al.*, 2005; *Kieffer et al.*, 2000; *Kieffer and Titus*, 2001; *Titus et al.*, 2001]. For example, we could limit the application of equation (1) between 85°S and 90°S and fix the rest of the values to those used in the controlled case. Because the mass in the residual cap is relatively small, it has little or no impact on the surface pressure, which is a measure of the total atmospheric mass. However, given the initial nature of this study, and the lack of a physical model for the geographical distribution of the albedo-insolation relationship, we think it is clearer here to explore the consequences of a simple, consistent relationship and to focus primarily on the ability of such a relationship to predict residual cap formation.

#### 3.3. Varying CO<sub>2</sub> Inventories With Insolation-Independent Albedo

[16] Using the time-constant (insolation-independent) albedo and emissivity values of the frost caps from the

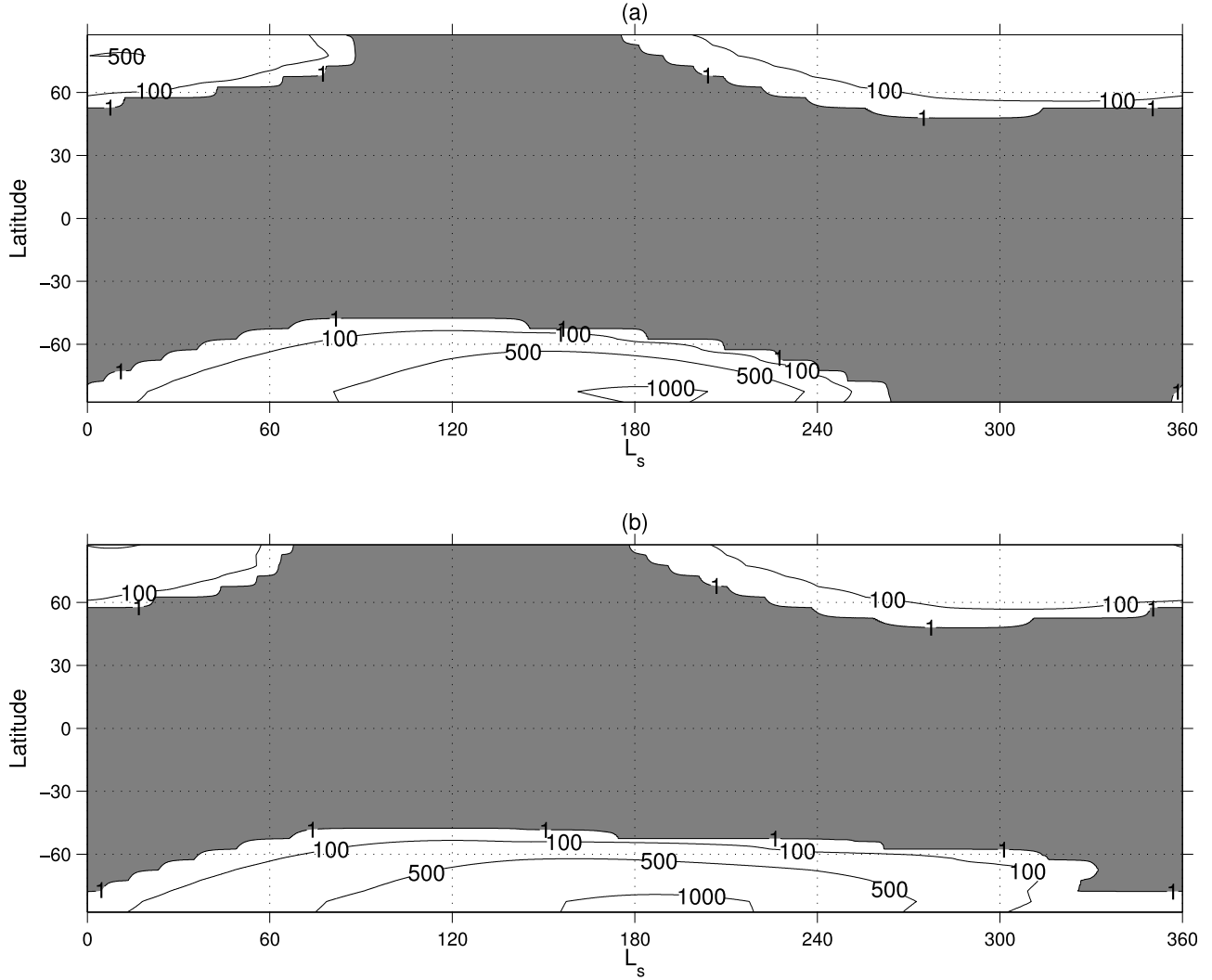


**Figure 2.** Annual variation of zonally averaged surface CO<sub>2</sub> ice deposition. The white background indicates the presence of surface CO<sub>2</sub> frost, while the grey background indicates the absence of it. The threshold is set to 1 kg m<sup>-2</sup>. From the edge of the polar cap in lower latitudes to the center of the cap, the grey contour lines indicate the deposition levels of 1 kg m<sup>-2</sup>, 100 kg m<sup>-2</sup>, 500 kg m<sup>-2</sup>, and 1000 kg m<sup>-2</sup>, respectively. (a) The control case, with time-constant CO<sub>2</sub> frost albedos and emissivities; the CO<sub>2</sub> inventory of the system is  $2.83 \times 10^{16}$  kg. (b) Same as Figure 2a, except the frost albedo is calculated using equation (1) in each time step.

control simulation, we experiment with different total CO<sub>2</sub> inventories. We vary the total mass from one third to 100 times the current amount. Associated surface CO<sub>2</sub> ice annual cycles are shown in Figure 4. In all cases, the model was begun with an initial condition subsurface temperature distribution generated from a multidecadal simulation at current mass and orbital parameters and with southern cap surface temperatures held at the CO<sub>2</sub> condensation point temperature. In this sense, the experiments are conservative in that the subsurface heat conduction is biased to favor a residual ice cap.

[17] The frost coverage patterns wax and wane from one experiment to another: while the latitudinal coverage does not change much, the surface ice densities increase then decrease as the total CO<sub>2</sub> inventory increases, as do the durations of the frost covering period in both hemispheres.

These variations are caused by two competing processes. First, increasing the total CO<sub>2</sub> inventory increases the (partial) pressure of CO<sub>2</sub> gas in the atmosphere. In response, the critical temperature for CO<sub>2</sub> condensation goes up (black solid line in Figure 6), which makes it easier for CO<sub>2</sub> to condense and persist as ice. Second, the enhanced greenhouse effect due to a denser atmosphere makes the planet warmer (grey line with diamonds in Figure 6), which tends to reduce CO<sub>2</sub> condensation. Therefore, when the first mechanism is dominating, adding to the total CO<sub>2</sub> inventory helps the formation of CO<sub>2</sub> frost in the winter (notice the increasing trend in the frost deposition in Figures 4a–4e). On the other hand, when the second mechanism is dominating, increasing the total CO<sub>2</sub> inventory reduces the formation of frost. The CO<sub>2</sub> surface frost amount decreases from Figure 4e to Figure 4h, and it completely disappears in

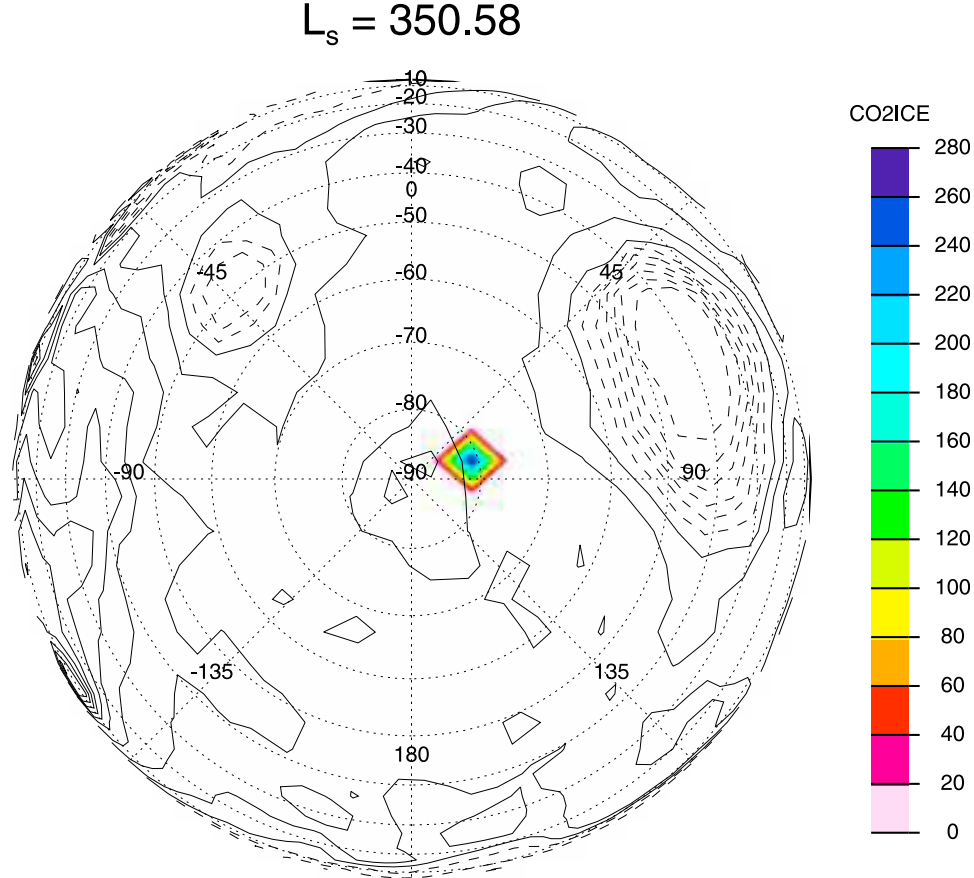


**Figure 3.** A snapshot of the southern hemisphere at  $L_s = 350.58$ . Color map represents the surface CO<sub>2</sub> ice abundance in kg m<sup>-2</sup>. Black contours indicate the Mars Orbiter Laser Altimeter topography data embedded in MarsWRF, with solid contours indicating positive values and dashed contours indicating negative values.

both hemispheres when we use 100 times the current mass (not shown in Figure 4). The transition CO<sub>2</sub> inventory separating these two regimes seems to be around 10 times the current inventory. Finally, we notice that none of these experiments predicts a perennial CO<sub>2</sub> ice cap.

### 3.4. Varying CO<sub>2</sub> Inventories With Insolation-Dependent Albedo

[18] We perform another set of experiments by combining the two modifications to MarsWRF described in sections 3.2 and 3.3. We change the CO<sub>2</sub> inventory while letting the CO<sub>2</sub> cap albedos respond to the incident solar flux following equation (1). The corresponding surface CO<sub>2</sub> ice annual variations are shown in Figure 5.

[19] Akin with the results found in section 3.3, the latitudinal coverage of the CO<sub>2</sub> frost does not change much. In general, for the same reasons, the frost deposition responds to the total CO<sub>2</sub> inventory similarly to what was described in section 3.3. More interesting differences are notable in the southern high latitudes. In the middle of the sequence of experiments, the CO<sub>2</sub> ice coverage is much greater and longevity is extended during southern summer. One can find a series of experiments that predict CO<sub>2</sub> ice persisting throughout the years (Figures 5b–5e). Some experiments

with higher inventory predict perennial caps in even lower latitudes (Figures 5c–5e). Again, the perennial CO<sub>2</sub> ice caps turn seasonal, even completely absent, when enough CO<sub>2</sub> gas is added to the system via the greenhouse effect of the CO<sub>2</sub>.

[20] These simulations suggest that the time-varying albedo is one of the decisive factors in predicting the perennial cap in GCMs. Although the increase of CO<sub>2</sub> critical temperature due to higher (partial) pressure helps the frost last longer in the spring and early summer, the environment is just not in sufficient energy deficit for ice to endure the entire summer with the kind of insolation or time-invariant albedo values typically used in models (see Figure 4). The enhanced albedos in the southern hemisphere create such energy deficits required by the perennial CO<sub>2</sub> frost, which is clearly demonstrated in Figure 6. Compared to the time-constant frost albedo (grey line with diamonds in Figure 6), the insolation-dependent albedo system has the effect of reducing near-surface temperature significantly as runs with successively more CO<sub>2</sub> are examined (black line with crosses in Figure 6). Eventually, the enhanced greenhouse effect overwhelms all other effects in the system and reduces and then prevents CO<sub>2</sub> ice cap formation (terminating them when roughly 100 times the current inventory is

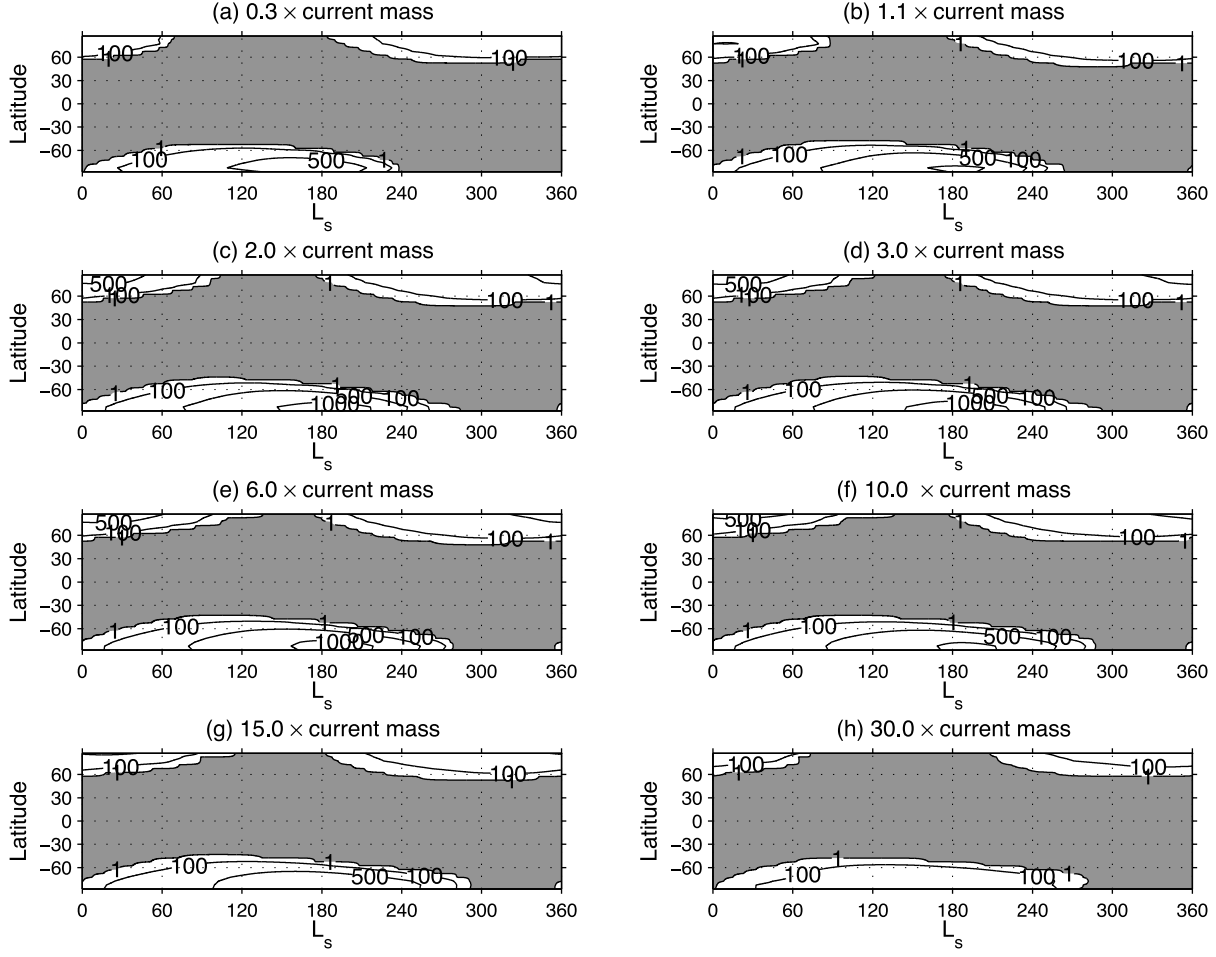


**Figure 4.** Annual variation of zonally averaged surface CO<sub>2</sub> deposition. Color scale and contour definition are the same as in Figure 2. Each plot corresponds to a different experiment with different total CO<sub>2</sub> inventory as specified in the plot titles. For these experiments, the frost albedos and emissivities are time constant and are fixed to the values used in the calibrated case (albedo of the northern cap is 0.795, emissivity of the northern cap is 0.485, albedo of the southern cap is 0.461, and emissivity of the southern cap is 0.785).

used). It is very interesting to notice that the current Martian atmospheric mass is just large enough to maintain one southern residual cap at its current latitude.

### 3.5. Influence of Obliquity on Residual Cap Formation and Location

[21] The secular perturbations due to all other planets in the solar system cause the orbit of Mars to change chaotically [Laskar, 1990]. Different orbital parameters, including spin axis obliquity and eccentricity, result in different patterns of surface insolation [Laskar *et al.*, 2002], which modify the CO<sub>2</sub> cycle by their direct impact on the surface energy balance. We experimented with different obliquity values, assuming this change would not cause any other surface properties to vary. We also used the present-day eccentricity and perihelion of the Martian orbit in these experiments. Corresponding surface CO<sub>2</sub> ice annual variations are shown in Figure 7.

[22] Figure 7 (left) shows the CO<sub>2</sub> ice cycles from simulations assuming the control case time-constant (insolation-independent) albedo. For low-obliquity simulations, the lack of incoming solar energy in the summer makes the polar region ideal for the CO<sub>2</sub> ice to persist through the local summer. For example, in the simulation with 10° obliquity (Figure 7a), permanent caps form at both poles. As the obliquity increases, seasonal CO<sub>2</sub> frost advances to lower latitudes as the location of the maximum reach of polar night extends equatorward. On the other hand, summer insolation becomes larger. Stronger sublimation reduces the amount and longevity of CO<sub>2</sub> frost and eventually eliminates the perennial cap (Figures 7c, 7e, and 7g). Again, the prediction from this class of models is that current Mars does not correspond to a state with a perennial CO<sub>2</sub> cap at either pole.

[23] If we assume the frost albedo responds to the solar insolation according to equation (1), the surface CO<sub>2</sub> ice cycles behave differently, as shown in Figure 7 (right). At

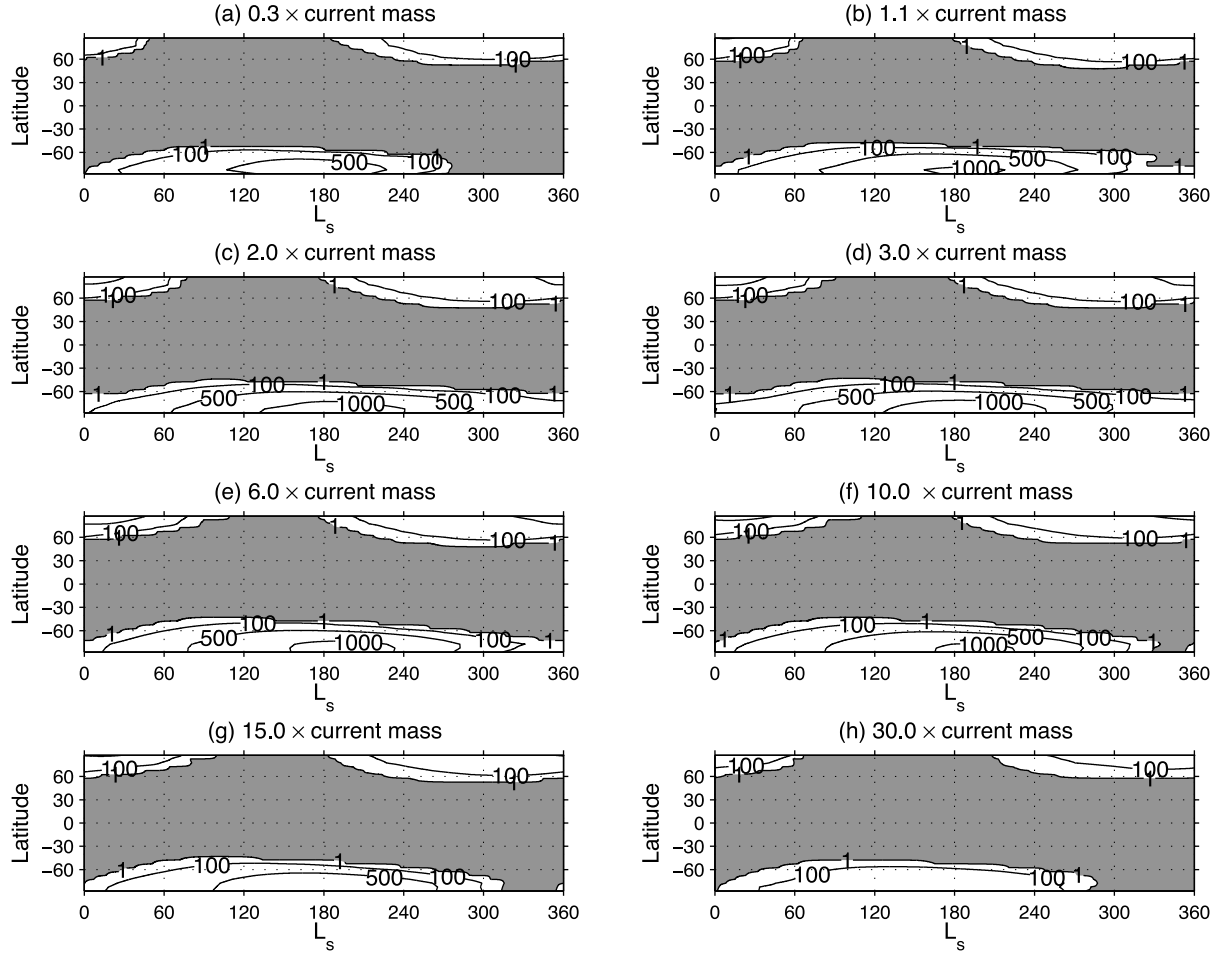


**Figure 5.** Same as Figure 4, except the CO<sub>2</sub> frost albedos are insolation-dependent according to equation (1).

low obliquity, we also find perennial CO<sub>2</sub> ice caps in both hemispheres for the same reasons described in section 3.4. As the obliquity increases, the effects of higher insolation (incoming energy) and higher albedo (outgoing energy) start to compete in the summer. Although slowly, summer CO<sub>2</sub> ice retreats in the southern polar region with increasing obliquity and reaches a minimum at an obliquity of 35° (Figure 7f). However, further increase of obliquity helps the albedo effect to gain dominance. At an obliquity of 45°, the summertime CO<sub>2</sub> ice is more extensive and thicker than at 35° (Figure 7h). The comparison between these two sets of experiments supports our argument that the response of the frost albedo to the solar insolation is crucial to predicting the permanent CO<sub>2</sub> ice cap. Furthermore, the insolation dependence may guarantee that the south would possess a residual CO<sub>2</sub> cap regardless of the obliquity if all other factors remained fixed (inventory, eccentricity, etc.).

### 3.6. Asymmetric Location of the Residual Cap

[24] Paige and Ingersoll [1985] and James *et al.* [1992] hypothesized that the time-varying and relatively high albedo of the southern residual cap must be related to ice

microphysical processes. However, geographical variations in the behavior were hard to explain without an understanding of what might cause geographical variations in the microphysical processes (or initial conditions). Colaprete *et al.* [2005] suggested that the skewed location of the perennial cap is due to the asymmetry in air temperatures during the formation of the ice cap, which is a consequence of the asymmetric atmospheric dynamics driven by the topography. They showed that the longitudinal climate asymmetry vanishes as Tharsis, Hellas, and Agyre are removed from the model. The longitudinal variations in air temperature map to differences in the fraction of surface CO<sub>2</sub> ice formed by direct deposition versus snowfall. While the model simulations shown by Colaprete *et al.* [2005] did not include any surface ice microphysics related to the deposition, the idea provides a solid concept of how microphysical evolution may vary geographically (in this case because small particles deposited as snow may evolve very differently from sheet ice deposited directly at the surface). Schmidt *et al.* [2009] also suggested that the asymmetry of the southern seasonal polar cap recession around the geographic south pole is only due to the albedo asymmetry.

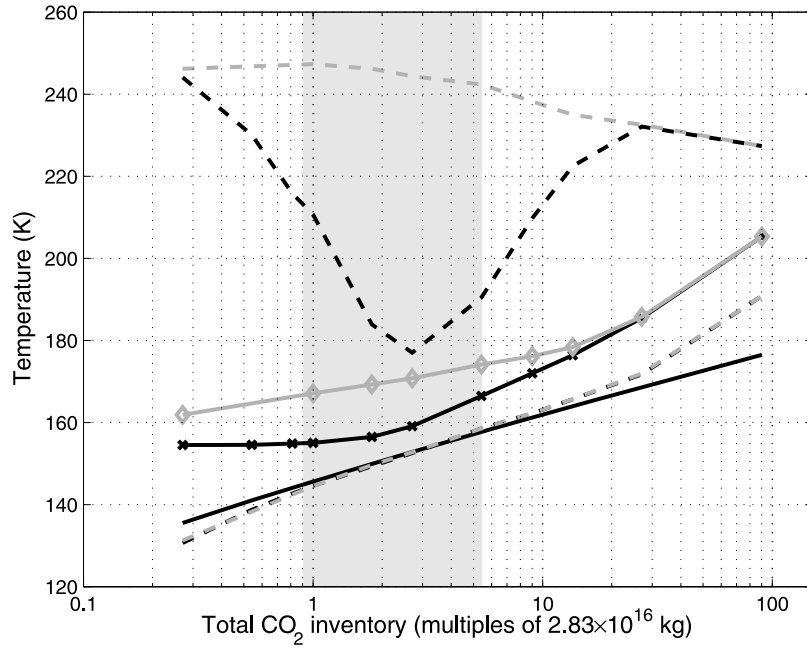


**Figure 6.** Annual near-surface atmospheric temperature variations near the south pole for experiments with different CO<sub>2</sub> inventories. The black solid line shows the critical temperature for CO<sub>2</sub> condensation. The grey line with open diamonds shows the annual average temperature for experiments with time-constant frost albedo (0.795 in the north, 0.461 in the south); the grey dashed lines indicate the temperature annual maxima and minima. The black line with crosses shows the annual average temperature for experiments with insolation-dependent frost albedo; the black dashed lines indicate the temperature annual maxima and minima. The shaded area covers the CO<sub>2</sub> inventories with which the MarsWRF predicts a southern perennial CO<sub>2</sub> cap if the CO<sub>2</sub> frost albedo is insolation-dependent.

[25] Assuming that the CO<sub>2</sub> frost albedo responds to the solar insolation according to equation (1), our model predicts a residual cap that is not symmetric in the longitudinal direction. Further simulations with MarsWRF show that surface boundary conditions, such as thermal inertia (or, equivalently, the subsurface heat conduction), surface slopes, and soil temperature, have very limited, if any, effects on the location of the perennial cap. On the other hand, changing the total CO<sub>2</sub> inventory or the obliquity of the planet results in migration of the location of the southern perennial cap (Figures 8 and 9). It is not clear why the location is sensitive to the inventory and obliquity, but changes in the spatial distribution of the surface energy balance resulting directly from these changes or indirectly via changes in the atmospheric circulation and its influence on the surface energy balance may be responsible. When we use the zonal averaged topography in MarsWRF, a zonally symmetric residual cap can be found at the south pole (see Figure 10). This is consistent with previous works, which suggest that the most important boundary condition that forces the circulation structure is the topography [Colaprete *et al.*, 2005; Richardson and Wilson, 2002a]. Mild asymmetry can still be found in the CO<sub>2</sub> ice distribution. It suggests that wave activity is also contributing, but those issues are beyond the scope of this paper. Nevertheless, the experiments above assert that the relationship between the perennial cap and the dynamic structure is very intimate, probably more so than with the surface properties.

### 3.7. Influence of Other Properties

[26] An important aspect of the current Martian climate system is that the CO<sub>2</sub> perennial cap dwells at the south pole. While the control case predicts no residual cap at all, a perennial cap is generated only for the south (Figure 2b) if we include the insolation-dependent albedo. However, there are issues with the control case that require some further investigation.

[27] There is a concern that the control case may bias against a northern cap because we used a relatively low emissivity (0.485) for this cap (although in reality, this low emissivity is merely aliasing the effects of subsurface heat transport associated with neglected subsurface water ice, and the resulting modeled surface energy balance, which is all that really matters here, is in fact rather close to that which is obtained on Mars [Guo *et al.*, 2009; Haberle *et al.*, 2004; Haberle *et al.*, 2008]). In any case, low emissivity reduces the energy that the cap gives away and therefore reduces the CO<sub>2</sub> condensation in winter and increases its sublimation in summer. We consequently performed a simulation in which we matched the northern CO<sub>2</sub> ice emissivity with that of the south (0.785). The resulting surface CO<sub>2</sub> ice cycle is shown in Figure 11a. As expected, the northern cap now contains more CO<sub>2</sub> ice with a longer lifetime. However, the increase of northern cap emissivity does not have sufficient impact to turn the northern seasonal cap into a perennial cap. Combined with the fact that we believe the low northern cap emissivity actually better

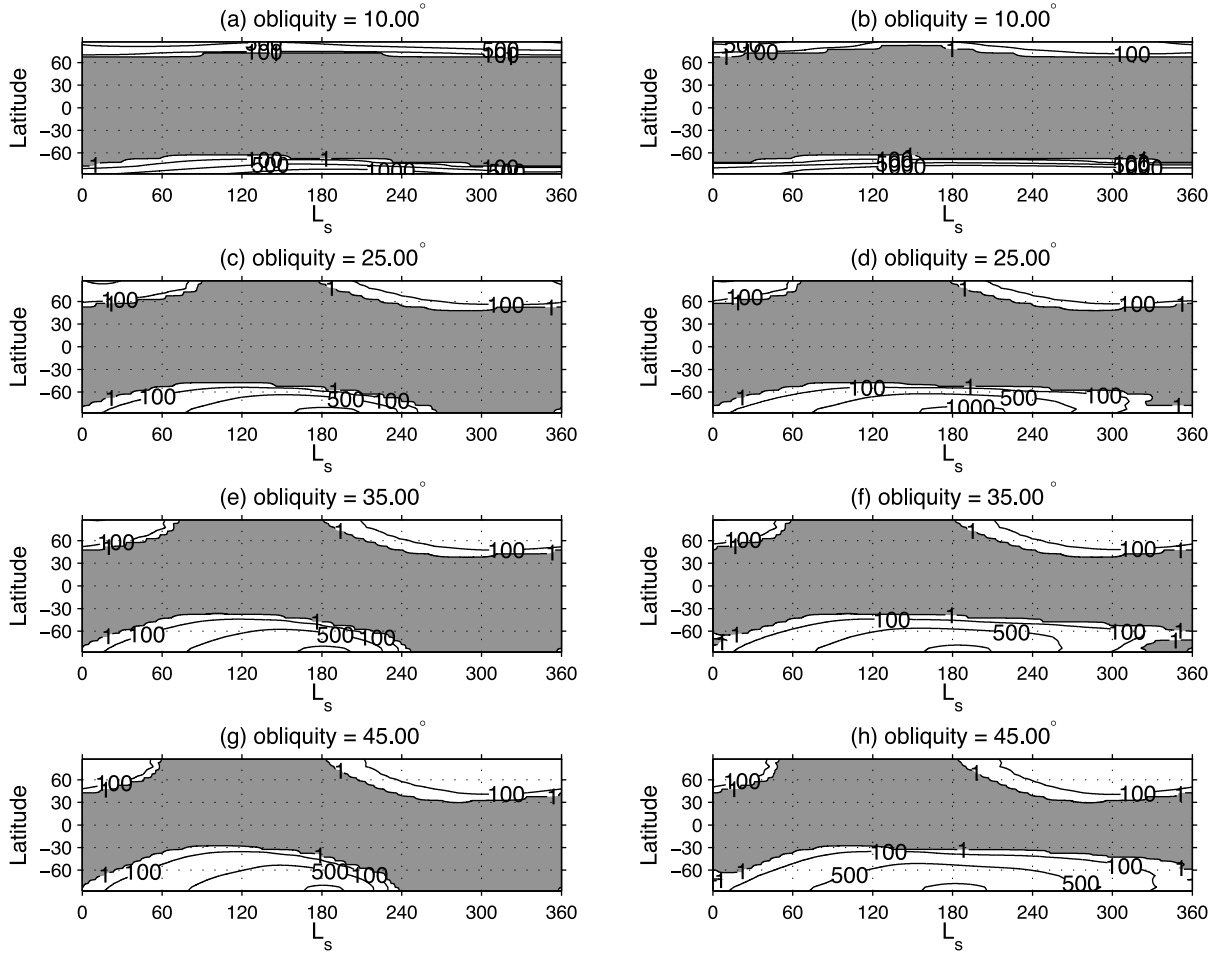


**Figure 7.** Annual variation of zonally averaged surface CO<sub>2</sub> deposition. Color scale and contour definition are the same as in Figure 2. Each plot corresponds to a different experiment with different obliquity as specified in the plot titles. (a, c, e, g) Simulations assuming controlled time-constant frost albedo (0.795 in the north and 0.461 in the south). (b, d, f, h) Simulations assuming insolation-dependent frost albedo.

represents the northern cap energy budget, these results suggest that a low northern cap emissivity is not responsible for the failure of the control case to generate a northern residual CO<sub>2</sub> ice cap.

[28] The thermal conductivity of the northern regolith may be higher than that of the southern regolith, which gives disadvantage to the northern hemisphere in retaining surface CO<sub>2</sub> ice [Guo et al., 2009; Haberle et al., 2008; Putzig et al., 2005]. In order to test the importance of the subsurface conductive heat, we performed an experiment in which we applied the global average regolith thermal conductivity at all locations (emissivities for CO<sub>2</sub> ice in both hemispheres were still set to 0.785). The corresponding surface CO<sub>2</sub> ice cycle is shown in Figure 11b. Little change can be found between Figures 11a and 11b. The north polar regolith in the control case has a relatively large thermal conductivity. Reducing the thermal conductivity increases the amount of CO<sub>2</sub> ice, but only slightly. The decrease of ice abundance in the southern summer is barely discernable where the thermal conductivity is raised. It confirms our argument that for this

magnitude of change, the subsurface heat conduction plays a less important role in the surface energy balance.

### 3.8. Influence of Argument of Perihelion and Eccentricity

[29] The current eccentricity of the orbit of Mars is relatively large (0.093), and given the timing of perihelion near the southern summer solstice, the insolation received in the two polar regions during their respective summers is very different. In the southern summer near the south pole, the insolation is up to 45% larger than that in the northern summer near the north pole. Such a difference projects an up to 0.2 difference in the insolation-dependent albedo using equation (1). This likely seems to be the decisive factor in explaining why the residual cap is located in the south. To examine this argument, we first set up a simulation in which the CO<sub>2</sub> ice albedo changes with insolation according to equation (1), the ice emissivity is fixed to 0.8, and the regolith thermal conductivity is set to the global average. When modeled with the current orbit of Mars, the resulting surface ice cycle is shown in Figure 11c. The pattern is very

## L<sub>s</sub> = 350.58 Surface

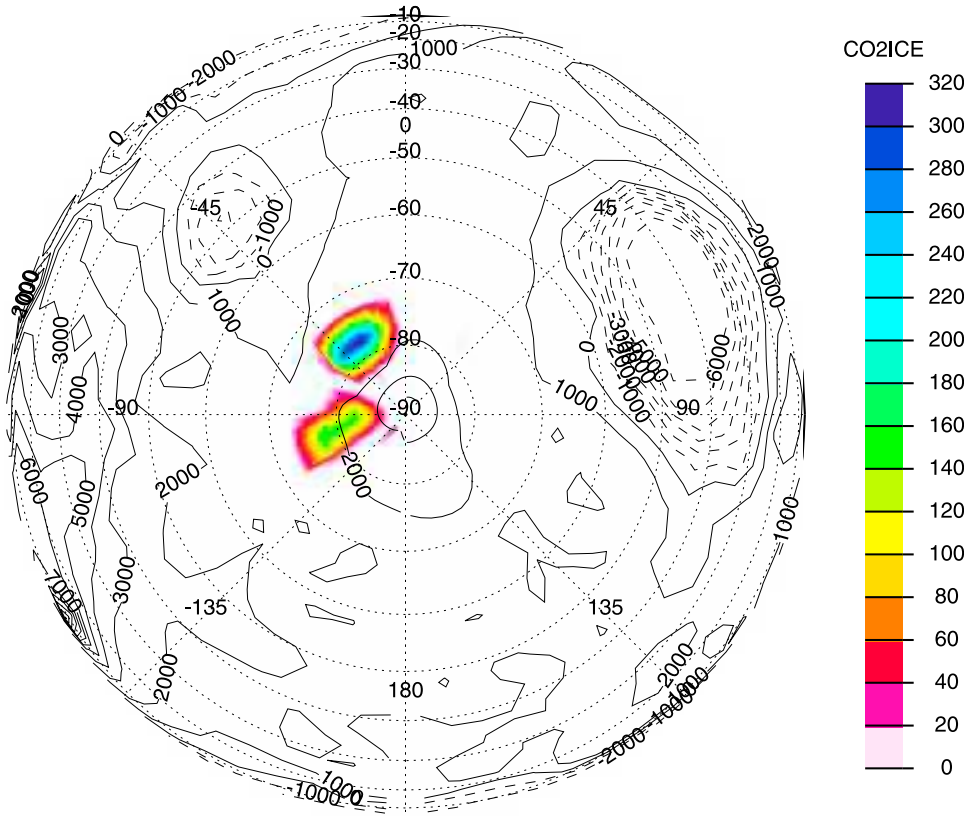


**Figure 8.** Same as Figure 3, except the total CO<sub>2</sub> inventory in this simulation is  $1.53 \times 10^{17}$  kg.

similar to what is shown in Figures 11a and 11b. We then performed another experiment, which has the same setup except that the timing of perihelion and aphelion are swapped by 180° relative to the present. Corresponding CO<sub>2</sub> ice annual variation is shown in Figure 11d. Now the northern polar region experiences much stronger insolation during its summer than does the south. As a result of equation (1), the northern cap yields higher ice albedo, and as a result a perennial cap is formed in the north. The situation for the southern polar region is exactly the opposite, causing the perennial ice to vanish in the southern summer. As a result, we are left with the rather counterintuitive result that the extremely volatile CO<sub>2</sub> ice more readily survives at the pole experiencing the more intense solsticial sunlight.

[30] One implication of our results is that if the CO<sub>2</sub> ice albedo follows the relationship indicated by equation (1), the existence of a perennial cap near the south pole is primarily dependent on the current orbit of Mars. If the orbit is different, and specifically the argument of perihelion, the pattern of the insolation annual variation will be different and the residual ice cap may switch to the opposite hemisphere. Interestingly, the physics of this control are opposite to those that control the location of the residual water ice cap (by the residual water ice cap, we mean the exposed water ice exchanging with the atmosphere, not the deeper polar layered deposits). For CO<sub>2</sub> stability, maximizing peak insolation is critical, while for water, it is minimizing insola-

tion that is key [Jakosky, 1983; Richardson and Wilson, 2002b]. As a result, we would expect water and CO<sub>2</sub> residual ice caps to swap hemispheres as the argument of perihelion progresses.

## 4. Conclusion and Discussion

[31] Viking data suggest an empirical linear relationship between the CO<sub>2</sub> ice cap albedo and the incident solar flux. When we include this relationship in MarsWRF, a GCM specifically designed for the study of the Martian atmosphere, we are able to reproduce a CO<sub>2</sub> cap that persists throughout the full year near the south pole. This perennial cap is not located exactly at the geographical south pole, nor is it zonally symmetric, which agrees with the observations. On the other hand, the predicted perennial cap is not at the same longitude as seen in the observations.

[32] As the atmospheric mass in the model initially increases, the condensation temperature for CO<sub>2</sub> increases, which makes it easier for CO<sub>2</sub> to condense and persist. However, the enhanced greenhouse effect introduced by the increase of the total atmospheric mass will ultimately outpace the increase of CO<sub>2</sub> critical temperature and will eventually prevent the presence of CO<sub>2</sub> frost in the summer (and eventually even in the winter). With increased CO<sub>2</sub> inventory, we still need the frost albedo responding to the sunlight as described by equation (1) in order to create a

## L<sub>s</sub> = 350.58 Surface

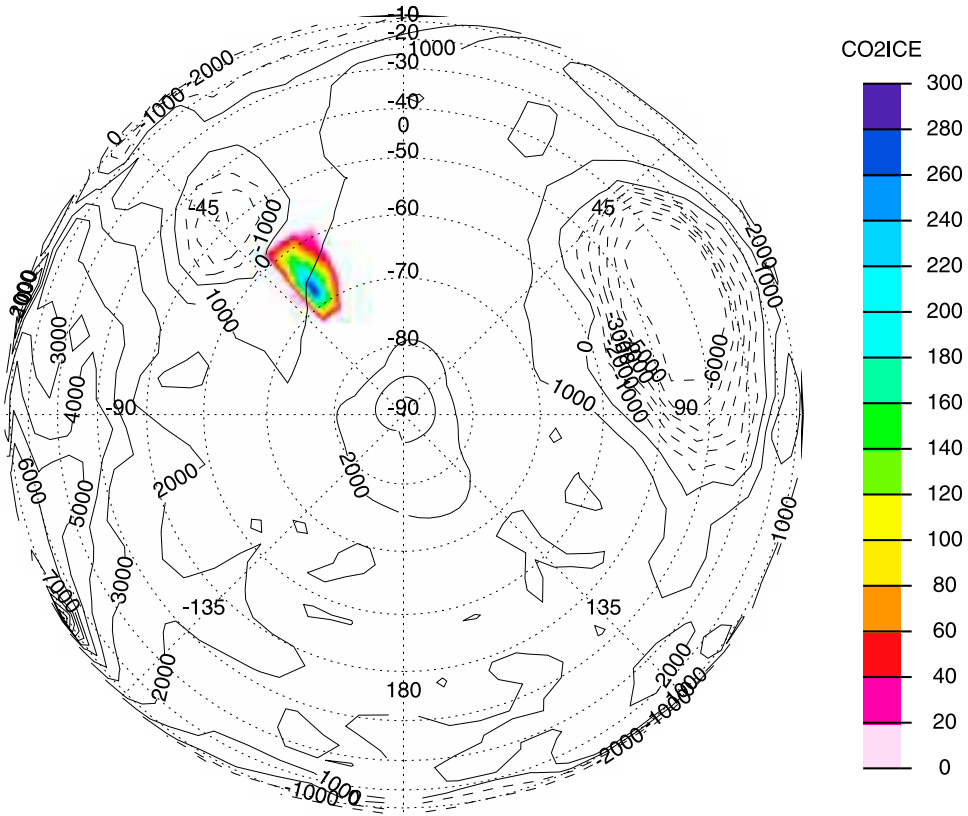


**Figure 9.** Same as Figure 3, except the obliquity of Mars in this simulation is 35°.

required energy deficit sufficiently large enough to form a perennial CO<sub>2</sub> ice cap. From our simulations, it is interesting to note that if the relationship between the surface CO<sub>2</sub> ice albedo and the incident solar flux holds, the current Martian atmospheric mass may be just large enough to maintain the southern residual cap at its current latitude. Obliquity is an important factor for determining the extents of the seasonal ice caps, but the formation of a residual southern cap is insensitive to obliquity when the albedo-insolation relationship is used. This is in marked contrast to the insolation-independent albedo simulations, where residual caps only form when the obliquity falls below roughly 15°, in agreement with prior studies [Newman *et al.*, 2005].

[33] Similar to other GCM studies of the perennial cap, none of our simulations were able to replicate the longitudinal location of the perennial cap asymmetry, as seen in the Viking observations. However, we did not include any spatial variation in the insolation dependence of the albedo that may result from the distribution of snowfall versus direct surface-deposited CO<sub>2</sub> ice [Colaprete *et al.*, 2005]. A “complete” model of the CO<sub>2</sub> ice caps, seasonal and perennial, will have to combine both the time-varying and spatially varying nature of the albedo, hopefully within the context of a physically based model of the CO<sub>2</sub> ice cap microphysics.

[34] Given the insolation dependence of the CO<sub>2</sub> ice albedo, the existence of a permanent CO<sub>2</sub> ice cap at the

south is related directly to the occurrence of peak insolation during southern rather than northern summer. It also requires the albedo-insolation function to increase the albedo sufficiently quickly with insolation that  $F_s(1 - a)$  decreases as  $F_s$  increases (where  $F_s$  is the insolation and  $a$  is the albedo). An important consequence of this function is a prediction that the residual CO<sub>2</sub> ice cap will switch hemispheres as the argument of perihelion progresses and alternately results in peak insolation in the north and the south. Interestingly, the CO<sub>2</sub> residual ice cap will be driven to the pole with highest peak insolation, while prior work on the Martian water cycle suggests that the residual water cap will always migrate to the pole with minimum peak summer insolation [Richardson and Wilson, 2002b]. Thus, Mars may remain with a very similar configuration of poles as we see it today (with just one CO<sub>2</sub> and one water), albeit periodically turned on its head as the perihelion timing changes.

[35] Data from various spacecraft and instruments, including Viking, MOC, TES, MOLA, and OMEGA, provide evidence for this monotonically increasing relationship between the albedo of the CO<sub>2</sub> ice cap and the insolation. Regardless of the details of the shape of the albedo-insolation function, as long as the slope of the curve is large enough, the fact that the albedo is an increasing function of the insolation is the key in explaining the existence of the perennial CO<sub>2</sub> ice cap and the cap’s preferential dwelling at the pole with higher peak insolation.

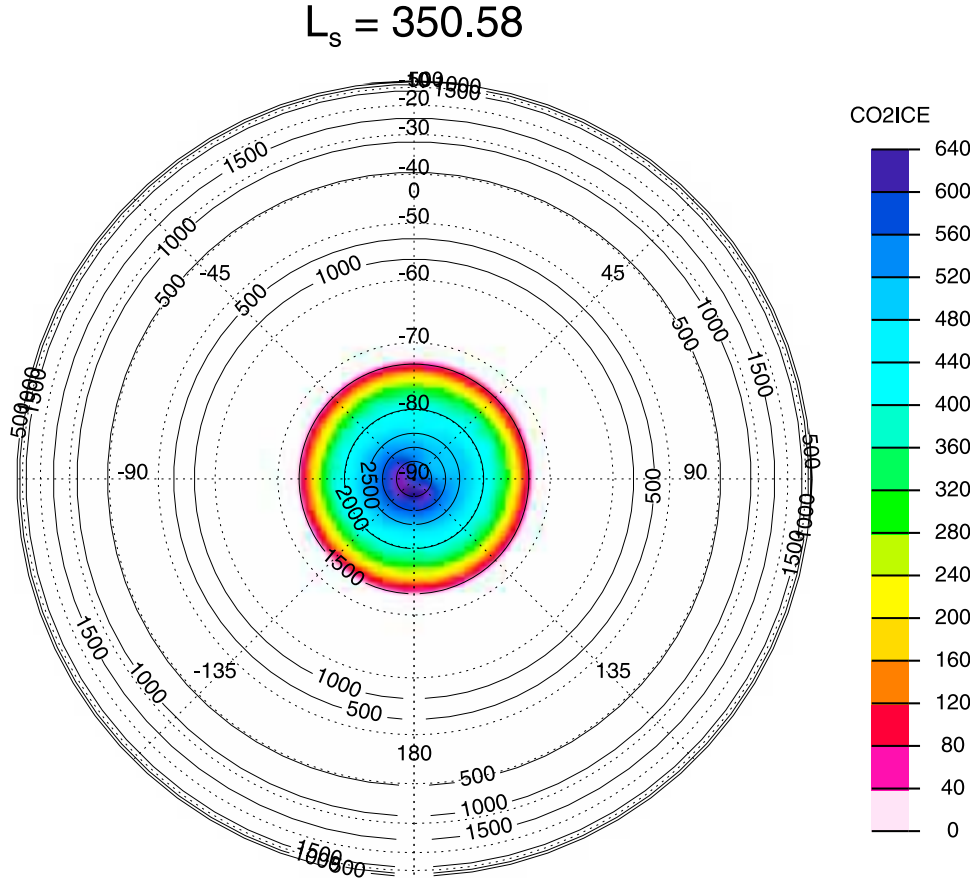


**Figure 10.** Same as Figure 3, except the zonal average value for topography and thermal inertia was used, and the total CO<sub>2</sub> inventory is  $1.53 \times 10^{17}$  kg.

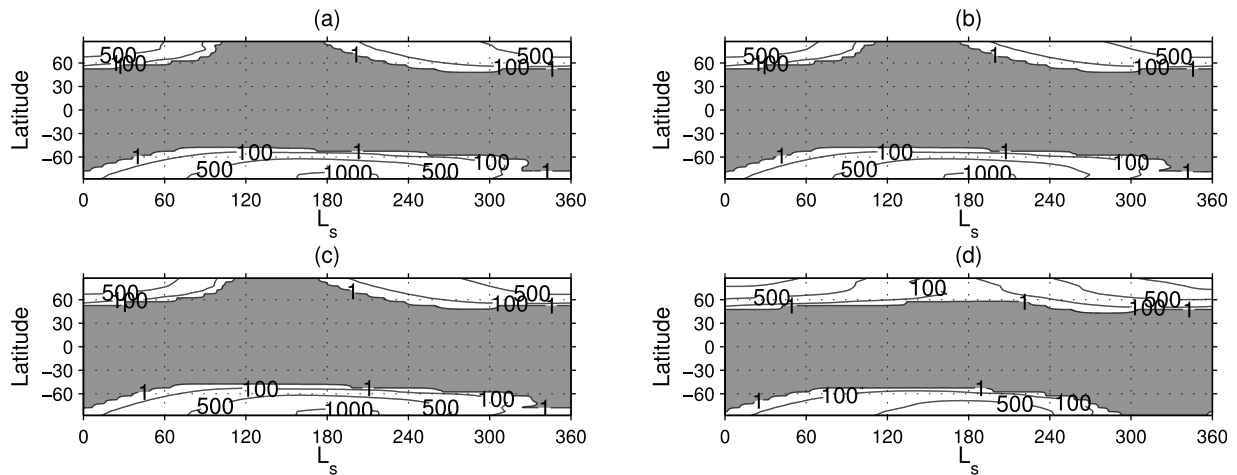


**Figure 11.** Annual variation of zonally averaged surface CO<sub>2</sub> deposition. Color scale and contour definition are the same as in Figure 2. (a) The zonal averaged CO<sub>2</sub> ice annual cycle for the simulation, which has the same setup as Figure 2b, except the northern cap albedo is set to 0.785. (b) The same setup as Figure 11a, except the regolith thermal inertia is set to the global average ( $216 \text{ J m}^{-3} \text{ K}^{-1}$ ). (c) An experiment in which the CO<sub>2</sub> ice albedo is decided by insolation according to equation (1), ice emissivity is set to 0.8, regolith thermal inertia is set to  $216 \text{ J m}^{-3} \text{ K}^{-1}$ , and the current orbital parameters for Mars are used. (d) An experiment whose setup is the same as for Figure 11c, except the perihelion and the aphelion are swapped.

[36] **Acknowledgments.** We thank Andrew Ingersoll and Kevin Lewis for useful discussions. We also thank two anonymous reviewers for their insightful comments. The numerical simulations for this research were performed on Caltech's Division of Geological and Planetary Sciences Dell cluster (CITerra).

## References

- Bibring, J. P., et al. (2004), Perennial water ice identified in the south polar cap of Mars, *Nature*, **428**, 627–630, doi:10.1038/nature02461.
- Byrne, S., and A. P. Ingersoll (2003), A sublimation model for Martian south polar ice features, *Science*, **299**, 1051–1053, doi:10.1126/science.1080148.
- Byrne, S., M. T. Zuber, and G. A. Neumann (2008), Interannual and seasonal behavior of Martian residual ice-cap albedo, *Planet. Space Sci.*, **56**(2), 194–211, doi:10.1016/j.pss.2006.03.018.
- Colaprete, A., J. R. Barnes, R. M. Haberle, J. L. Hollingsworth, H. H. Kieffer, and T. N. Titus (2005), Albedo of the south pole on Mars determined by topographic forcing of atmosphere dynamics, *Nature*, **435**, 184–188, doi:10.1038/nature03561.
- Forget, F., F. Hourdin, and O. Talagrand (1998), CO<sub>2</sub> snowfall on Mars: Simulation with a general circulation model, *Icarus*, **131**, 302–316, doi:10.1006/icar.1997.5874.
- Forget, F., F. Hourdin, R. Fournier, C. Hourdin, O. Talagrand, M. Collins, S. R. Lewis, P. L. Read, and J. P. Huot (1999), Improved general circulation models of the Martian atmosphere from the surface to above 80 km, *J. Geophys. Res.*, **104**, 24,155–24,175, doi:10.1029/1999JE001025.
- Guo, X., W. G. Lawson, M. I. Richardson, and A. D. Toigo (2009), Fitting the Viking Lander surface pressure cycle with a Mars general circulation model, *J. Geophys. Res.*, **114**, E07006, doi:10.1029/2008JE003302.
- Haberle, R. M., B. Mattingly, and T. N. Titus (2004), Reconciling different observations of the CO<sub>2</sub> ice mass loading of the Martian north polar cap, *Geophys. Res. Lett.*, **31**, L05702, doi:10.1029/2004GL019445.
- Haberle, R. M., F. Forget, A. Colaprete, J. Schaeffer, W. V. Boynton, N. J. Kelly, and M. J. Chamberlain (2008), The effect of ground ice on the Martian seasonal CO<sub>2</sub> cycle, *Planet. Space Sci.*, **56**(2), 251–255, doi:10.1016/j.pss.2007.08.006.
- Ingersoll, A. P., T. Svitak, and B. Murray (1992), Stability of polar frosts in spherical bowl-shaped craters on the Moon, Mercury, and Mars, *Icarus*, **100**, 40–47, doi:10.1016/0019-1035(92)90016-Z.
- Jakosky, B. M. (1983), The role of seasonal reservoirs in the Mars water cycle: II. Coupled models of the regolith, the polar caps, and atmospheric transport, *Icarus*, **55**, 19–39, doi:10.1016/0019-1035(83)90047-7.
- James, P. B., H. H. Kieffer, and D. A. Paige (1992), The seasonal cycle of carbon dioxide on Mars, in *Mars*, edited by H. H. Kieffer et al., pp. 934–968, Univ. of Ariz. Press, Tucson.
- Kelly, N. J., W. V. Boynton, K. Kerry, D. Hamara, D. Janes, R. C. Reedy, K. J. Kim, and R. M. Haberle (2006), Seasonal polar carbon dioxide frost on Mars: CO<sub>2</sub> mass and columnar thickness distribution, *J. Geophys. Res.*, **111**, E03S07, doi:10.1029/2006JE002678 [printed 112(E3), 2007].
- Kieffer, H. H. (1979), Mars south polar spring and summer temperature: A residual CO<sub>2</sub> frost, *J. Geophys. Res.*, **84**, 8263–8288, doi:10.1029/JB084B14p08263.
- Kieffer, H. H., and T. N. Titus (2001), TES mapping of Mars' north seasonal cap, *Icarus*, **154**, 162–180, doi:10.1006/icar.2001.6670.
- Kieffer, H. H., T. Z. Martin, A. R. Peterfreund, B. M. Jakosky, E. D. Miner, and F. D. Palluconi (1977), Thermal and albedo mapping of Mars during the Viking primary mission, *J. Geophys. Res.*, **82**, 4249–4291, doi:10.1029/JS082i028p04249.
- Kieffer, H. H., T. N. Titus, K. F. Mullins, and P. R. Christensen (2000), Mars south polar spring and summer behavior observed by TES: Seasonal cap evolution controlled by frost grain size, *J. Geophys. Res.*, **105**, 9653–9699, doi:10.1029/1999JE001136.
- Laskar, J. (1990), The chaotic motion of the solar system. A numerical estimate of the size of the chaotic zones, *Icarus*, **88**, 266–291, doi:10.1016/0019-1035(90)90084-M.
- Laskar, J., B. Levrard, and J. F. Mustard (2002), Orbital forcing of the Martian polar layered deposits, *Nature*, **419**, 375–377, doi:10.1038/nature01066.
- Newman, C. E., S. R. Lewis, and P. L. Read (2005), The atmospheric circulation and dust activity in different orbital epochs on Mars, *Icarus*, **174**, 135–160, doi:10.1016/j.icarus.2004.10.023.
- Owen, T., K. Biemann, D. R. Rushneck, J. E. Biller, D. W. Howarth, and A. L. Lafleur (1977), The composition of the atmosphere at the surface of Mars, *J. Geophys. Res.*, **82**, 4635–4639, doi:10.1029/JS082i028p04635.
- Paige, D. A. (1985), The annual heat balance of the Martian polar caps from Viking observations, Ph.D. thesis, Calif. Inst. of Technol., Pasadena.
- Paige, D. A. (1992), The thermal stability of near-surface ground ice on Mars, *Nature*, **356**, 43–45, doi:10.1038/356043a0.
- Paige, D. A., and A. P. Ingersoll (1985), Annual heat balance of the Martian polar caps: Viking observations, *Science*, **228**, 1160–1168, doi:10.1126/science.228.4704.1160.
- Paige, D. A., K. E. Herkenhoff, and B. C. Murray (1990), Mariner-9 observations of the south polar cap of Mars: Evidence for residual CO<sub>2</sub> frost, *J. Geophys. Res.*, **95**, 1319–1335, doi:10.1029/JB095iB02p01319.
- Pollack, J. B., R. M. Haberle, J. R. Murphy, J. Schaeffer, and H. Lee (1993), Simulations of the general circulation of the Martian atmosphere: 2. Seasonal pressure variations, *J. Geophys. Res.*, **98**, 3149–3181, doi:10.1029/92JE02947.
- Putzig, N. E., M. T. Mellon, K. A. Kretke, and R. E. Arvidson (2005), Global thermal inertia and surface properties of Mars from the MGS mapping mission, *Icarus*, **173**, 325–341, doi:10.1016/j.icarus.2004.08.017.
- Richardson, M. I., and R. J. Wilson (2002a), A topographically forced asymmetry in the Martian circulation and climate, *Nature*, **416**, 298–301, doi:10.1038/416298a.
- Richardson, M. I., and R. J. Wilson (2002b), Investigation of the nature and stability of the Martian seasonal water cycle with a general circulation model, *J. Geophys. Res.*, **107**(E5), 5031, doi:10.1029/2001JE001536.
- Richardson, M. I., A. D. Toigo, and C. E. Newman (2007), PlanetWRF: A general purpose, local to global numerical model for planetary atmospheric and climate dynamics, *J. Geophys. Res.*, **112**, E09001, doi:10.1029/2006JE002825.
- Schmidt, F., S. Doute, B. Schmitt, M. Vincendon, J.-P. Bibring, Y. Langevin, and the OMEGA Team (2009), Albedo control of seasonal south polar cap recession on Mars, *Icarus*, **200**, 374–394, doi:10.1016/j.icarus.2008.12.014.
- Tillman, J. E., N. C. Johnson, P. Guttorp, and D. B. Percival (1993), The Martian annual atmospheric pressure cycle: Years without great dust storms, *J. Geophys. Res.*, **98**, 10,963–10,971, doi:10.1029/93JE01084.
- Titus, T. N., H. H. Kieffer, K. F. Mullins, and P. R. Christensen (2001), TES premapping data: Slab ice and snow flurries in the Martian north polar night, *J. Geophys. Res.*, **106**, 23,181–23,196, doi:10.1029/2000JE001284.
- Wood, S. E., and D. A. Paige (1992), Modeling the Martian seasonal CO<sub>2</sub> cycle 1. Fitting the Viking Lander pressure curves, *Icarus*, **99**, 1–14, doi:10.1016/0019-1035(92)90166-5.

X. Guo and A. Soto, Planetary Science, Division of Geological and Planetary Sciences, California Institute of Technology, 1200 E. California Blvd., MC150-21, Pasadena, CA 91125, USA. (xin@gps.caltech.edu)

M. I. Richardson, Ashima Research, 600 S. Lake Ave., Pasadena, CA 91106, USA.

A. Toigo, Center for Radiophysics and Space Research, Cornell University, 326 Space Sciences Bldg., Ithaca, NY 14853, USA.